

# MODELING PROBE AND TISSUE INTERACTION FOR TUMOR FEATURE EXTRACTION

**Parris S. Wellman**

**Robert D. Howe**

Division of Engineering and Applied Sciences  
Harvard University  
Cambridge, Massachusetts

## 1 INTRODUCTION

Fingertip palpation is performed widely to detect tumors embedded in soft tissue. It is used to locate tumors in the lung for excision, and to detect and characterize tumors in the breast for diagnosis. However, it can be difficult to reliably locate these masses and estimate their properties. We are developing a system that uses a mechanical probe to document the locations and properties of these tumors. This system will make non-invasive pressure measurements on the surface of the probe as it is indented into the tissue (Howe et al, 1995). Relating these measurements to the properties of the tissue and the tumor requires a model of the tissue-probe interaction.

This paper presents a model for determining the stress profile along the surface of a curved probe contacting a tissue layer of finite thickness containing an inclusion. This is a reasonable analogy to typical clinical situations (e.g. tumors in lung and breast tissue). The ultimate goal is to invert this model to estimate the size, stiffness, location and depth of tumors embedded in real tissue using the pressure measurements made on the surface of a probe.

Previous work on this problem is limited to analysis of the contact of two homogeneous elastic bodies (Johnson 1985) or the effect of a rigid inclusion in infinite (Eshelby 1957) or joined semi-infinite (Yu 1991) solids. Since the problem of the contact of a curved probe with a finite tissue layer containing an inclusion is not tractable analytically, we have used the finite element method for its analysis.

## 2 METHODS

Real lung and breast tissue are often of relatively uniform thickness and large extent when compared to the probe size. As an approximation to this case we have chosen a model sufficiently wide that edge effects may be ignored. However, the finite thickness of the tissue is important and this condition is retained in the model. For this initial study we have used a plane strain formulation that incorporates large deformations and finite strain. Figure 1 shows the two dimensional model that was

analyzed using the ABAQUS finite element analysis package. In this model,  $R$  is the radius of the probe,  $r$  is the radius of the tumor,  $h$  is the depth of the tumor and  $2h$  is the thickness of the tissue. We have assumed that the tissue and tumor are isotropic and elastic, thus  $E_1$  and  $E_2$  are the Young's moduli for the tumor and tissue respectively, while the Poisson ratio was taken to be 0.49 for both. The probe is assumed to be rigid so it can be located by the apex coordinates  $x$  and  $y$  in the lateral and indentation directions. For the analysis presented here, we have chosen  $r/R=0.5$  and  $h/R=1.0$  because these ratios are similar to those at the limit of human ability to detect tumors during palpation. For this first model we have ignored dynamic effects.

## 3 RESULTS

Figure 2 shows the results of four indentation models at  $E_1/E_2=1$  (no tumor), and  $E_1/E_2 = 10, 100$  and  $1000$ . In these trials, the hemi-cylindrical probe was indented to  $y/R$

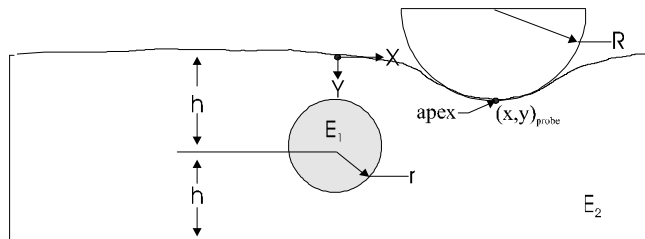


Figure 1 Geometry of the Finite Element Model

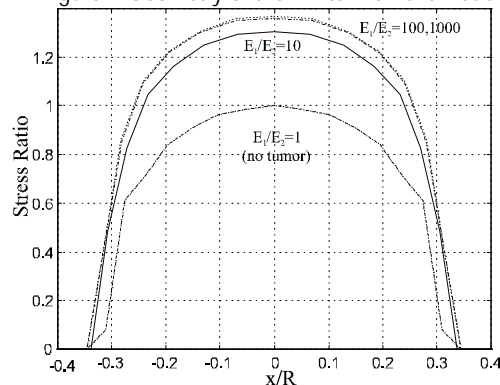


Figure 2 - Stress Profile on Surface of Probe at  $y/R = 0.4$ .

= 0.4. The stress ratio was calculated for this figure and in all subsequent figures by normalizing the stress values with the peak stress on the probe when it was indented into tissue with no tumor. The figure shows that while the overall magnitude of the stress changes, the shape does not change significantly. This figure also shows that the surface stress distribution is symmetric when the probe is indented into tissue that does not contain a tumor.

Figure 3 shows the stress ratio on the face of the probe for  $x/R = -0.625, 0$  and  $0.625$  with  $y/R = 0.4$  and  $E_1/E_2 = 1000$ . The figure shows that the stress distribution is symmetric when the probe is directly over the center of the tumor ( $x/R = 0$ ), but that it becomes asymmetric when the probe and tumor are not aligned. Also, the highest stress on the probe is not at the apex of the probe, but rather at another point.

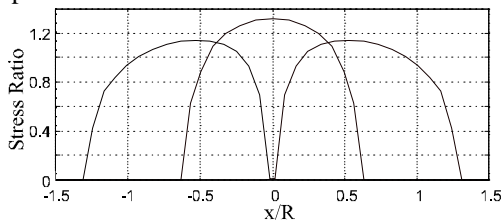


Figure 3 - Probe Stress Profiles for 3 Indentation Positions

#### 4 DISCUSSION

We are interested in obtaining estimates of the size, shape, location and stiffness of tumors from pressure distribution measurements made on the face of a probe. Figure 2 makes it clear that little information about the features of a tumor can be ascertained from a single static measurement centered over the tumor because there is little difference in the shape of the curves which would be unnoticeable in the presence of noise. These small differences in pressure curve shape also make it difficult to distinguish between an indentation test with a tumor beneath the surface and an indentation test performed on tissue that has a higher stiffness. Since we are interested in extracting tumor features that another approach must be used to obtain this information.

Figure 3 shows that there is asymmetry in the pressure profile when a tumor is present in the tissue and the probe is not centered over it. These two figures demonstrate that it is necessary to consider a series of distributions measured as the probe slides across the tissue surface rather than a single distribution from a static indentation test. By comparing these multiple frames, and measuring the location of the probe during each, it should be possible to estimate various properties of the tumor.

Figure 4(a) shows the normal pressure at the apex of the probe taken from a sequence of computations as it slides from  $\Delta x/R = 1.5$  to  $\Delta x/R = -1.5$  with  $E_1/E_2 = 1000$ . The stress ratio goes to 1 at the ends of the curve, while it reaches a high of 1.32 directly over the tumor. It is possible to

develop a variety of discrimination functions based on this curve. For this study we have concentrated on finding the location of the center of the tumor.

One possibility is to look at the pressure at the apex of the probe (as in Figure 4(a)) and find its peak. Because this is a single point measurement it will be susceptible to signal noise, and thus more robust discrimination methods are desirable. A simple example is motivated by observing that the pressure distribution shown in Figure 3 is symmetric when the probe apex is directly over the center of the tumor, but that it is asymmetric when it is partially over the tumor. This implies that as the probe passes over the tumor some torque will be required to keep it from rotating. We define one possible discrimination function,

$$D(x/R) = \frac{\text{Right Side Pressure Moment}}{\text{Left Side Pressure Moment}} = \frac{\int_{x=x_{apex}}^{x=x_{apex}+r} P(x-x_{apex})(x-x_{apex})dx}{\int_{x=x_{apex}-r}^{x=x_{apex}} P(x-x_{apex})(x-x_{apex})dx} \quad (1)$$

where  $x_0$  is the  $x$  coordinate of the apex of the probe. This measure is related to the total torque acting on the right side of the probe divided by the total torque acting on the left side of the probe. Figure 4(b) shows that this function crosses 1 when the probe tip crosses the center of the tumor which can be used to estimate its location. Since this function integrates the value of the pressure across the surface of the probe, noise on the signal will tend to be averaged, making this function more robust than the first measure. More sophisticated discrimination functions that take noise properties into account are under development.

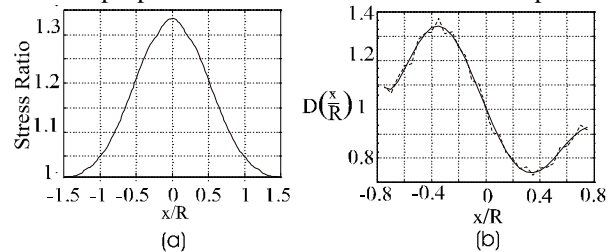


Figure 4 - (a) Probe Apex Stress (b) Stress Moment. Both During Sliding from  $x/R = 0.5$  to  $-0.5$ . ( $y/R = 0.4, r/R = 0.5, h/R = 1, E_1/E_2 = 1000$ )

In future work we will examine the effects on the output of varying the geometric and stiffness ratios in the model. Finally, we observe that even though multiple pressure images are essential to determine tumor and tissue properties, dynamic (viscoelastic) effects may provide even more information. We will consider dynamic effects in subsequent models.

#### REFERENCES

Eshelby, J.D. The determination of the elastic field of an ellipsoidal inclusion and related problems. *Proc. R. Soc. Lond., A* 241:376-396. 1957.

Howe, R.D. et als. Remote Palpation Technology. *IEEE Eng. in Med. and Biology.* 14.3. IEEE. May/June 1995.

Johnson, K.L. *Contact Mechanics.* Camb. U. Press. 1985

Yu, H.Y. and Sanday, S.C. Elastic field in joined semi-infinite solids with an inclusion. *Proc. R. Soc. Lond.* A 434:521-530. 1991.